

# Coupling Temperature Distribution with the Single Particle Model

Matthew Hunt<sup>d</sup>, Florian Theil<sup>b</sup>, Ferran Brosa Planella<sup>b,c</sup>, W. Dhammika Widanage<sup>1a,c</sup>

<sup>a</sup>WMG, University of Warwick, Coventry CV4 7AL

<sup>b</sup>Mathematics Institute, Zeeman Building, University of Warwick, Coventry CV4 7AL

<sup>c</sup>The Faraday Institution, Quad One, Becquerel Avenue, Harwell Campus, Didcot, OX11 0RA

<sup>d</sup>Qdot Technology, Office F20 Atlas Building R27 Rutherford Appleton Laboratory Harwell, Didcot OX11 0QX

---

## Abstract

The DFN (Doyle-Fuller-Newman) model is well known for being accurate and computationally expensive. In situations where temperature gradients are important (eg fast charging) it is desirable to couple the temperature dynamics within a battery into the DFN model. This leads to even greater computational complexity. Inspired by the work of Marquis et al [1] we present the derivation of a reduced-order model based on the DFN model with temperature in the macroscale. The complexity of the reduced-order model is characterised by the local temperature plus one internal electro-chemical dimension and the electrolyte dynamics is accounted for by a simple correction term.

*Keywords:* Lithium-ion batteries, Temperature effects

---

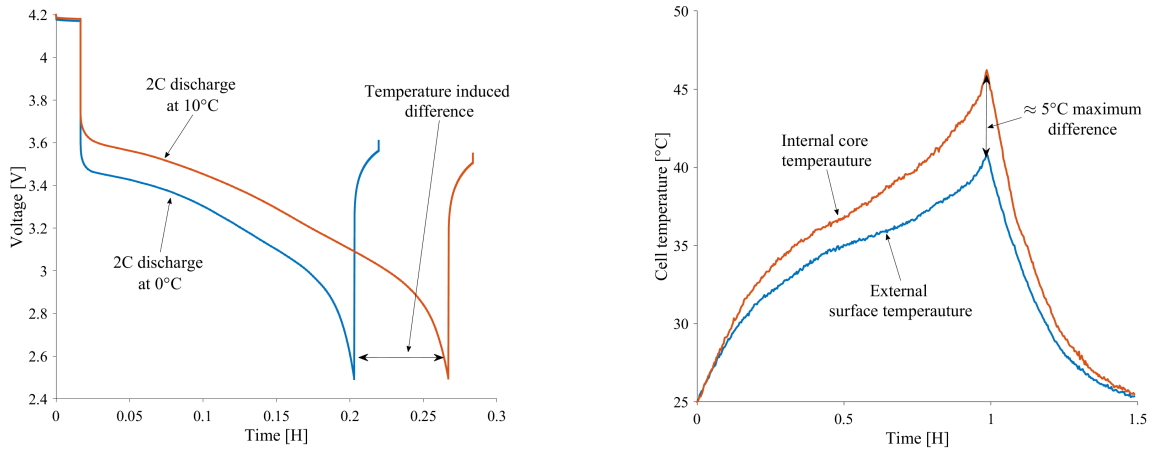
## 1. Introduction

With the rise of intermittent energy resources (wind, tidal and wave to mention a few) as well as the rise of electric and hybrid cars, there is a need to develop batteries with higher capacities, and the dominant technology is the lithium-ion battery. The modelling of lithium-ion batteries was initiated with the seminal paper by Doyle, Fuller and Newman [2, 3, 4] which established the model known as the Doyle-Fuller-Newman (DFN) model. Although this model included temperature as a parameter, it ignored the dynamics of temperature based upon electrochemistry. When the battery is operated at a small C-rate, the temperature effects are relatively minor and the DFN model provides a good description of the charge/discharge process. At higher C-rates, the rise in temperature and its effects on the electrochemical properties are no longer negligible and the DFN model needs to be extended to account for them. Moreover, these changes in temperature enhance battery degradation [5], and these effects are particularly important in applications such as electric vehicles.

Electric vehicles are developing sophisticated thermal management systems. For example, the Toyota Prius relied on passive air cooling, while the latest Tesla Models rely on active liquid cooling design [6]. Such thermal management systems rely on knowing the internal cell temperature distribution and its dynamics since they influence the design choices of the cooling arrangements (e.g. surface or tab cooling with cooling plates or use of immersed cooling etc.).

Knowing the internal cell temperature dynamics also allows effective control algorithms to be developed to maintain a low temperature gradient ( $\leq 5^\circ\text{C}$ ) both inside a cell and between the cells within a module [7]. Maintaining such low thermal gradients is crucial to ensure pack safety and minimise battery degradation.

Two measurement examples are provided below that show a typical gradient and the impact of ambient temperature on cell performance. Figure (1a) demonstrates the increase in resistance when the ambient temperature of a commercial battery (5Ah NMC811 21700 cell [8]) is cooled ( $0^\circ\text{C}$  compared to  $10^\circ\text{C}$ ). The cells on this occasion were thermally controlled in oil baths and a constant current discharge of 2C was applied. The voltage response while at  $0^\circ\text{C}$  has a larger drop in potential and reaches the cut-off terminal voltage of 2.5V much earlier than when at  $10^\circ\text{C}$ . This is due to the conductivity and diffusivity of the electrodes and electrolyte becoming less favourable when at lower temperatures (usually following an Arrhenius behaviour, [9, 10]). Similarly Figure (1b) demonstrates a typical temperature difference that occurs between the core of a cell (cylindrical) against the cell surface. The cell was placed in a thermal chamber with a set-point of  $25^\circ$  with forced convection and discharged at 1C. A maximum difference of approximately  $5^\circ\text{C}$  is observed by the end of the discharge. The induced gradients will therefore lead to varied electrochemical kinetics (in the radial direction of the cell), which over a long period of use, will cause inhomogeneous ageing of the different layers within the cell.



(a) Influence of ambient temperature on a 2C discharge voltage response. The cells were thermally controlled at  $0^\circ\text{C}$  and  $10^\circ\text{C}$  in an oil bath.

(b) Temperature gradient build up in a cell when discharged at 1C at  $25^\circ\text{C}$  ambient. The cell was thermally controlled in a thermal chamber with forced convection.

Figure 1: Voltage and thermal responses of a commercial 5 Ah 21700 cylindrical cell. The chemistry of the positive electrode is NMC811 while in the negative electrode it is graphite and silicon oxide. More details on this cell can be found in [8].

### 1.1. Our contribution

The aim of this paper is to present an effective, physics-based model which tracks

- The temperature distribution within the battery.
- Lithium concentration in the electrodes.
- Lithium concentration in the electrolyte.

The model can be viewed as an extension of the SPMe model by Marquis et al. [1] by including temperature as a dynamic variable. Here we provide a derivation via asymptotic expansion from the a standard DFN model with temperature, cf [11].

### 1.2. Literature review

The literature on temperature dynamics of a lithium ion battery is less developed than the account of electrochemical models. Depending on their level of accuracy, models either capture average temperatures or spatially resolved temperatures. There are three scales involved in battery modelling: the microscale, which is where the lithium ions diffuse in and out of the electrode particles; the mesoscale where the negative electrode, separator and positive electrode are considered (sometimes also called the *cell level*); and the macroscale, which is the physical battery, a typically cylindrical, pouch cell or prismatic battery.

One of the first comprehensive approaches to write down a temperature equation for a lithium-ion battery was put forward in the seminal paper by Gu and Wang [13] in 2000. The resulting model is for temperature on the mesoscale which is of the form of a general parabolic temperature equation with four source terms representing Ohmic heating in the solid phase, electrolyte, reversible and irreversible heating. The source terms are coupled to equations in the mesoscale in the form of the electric potentials.

The paper [14] presents a systematic derivation of a temperature for the macroscale and mesoscale. This is a comprehensive physics-based model which includes four heat source terms in the mesoscale and macroscale. An asymptotic reduction is carried based upon different timescales.

There are a number of lumped parameter models, [15] where the temperature is assumed to be homogeneous. The equation for temperature is an ordinary differential equation (ODE) rather than a partial differential equation (PDE), so temperature gradients within the battery on the macroscale are ignored. The models usually consider radiation and convection as mechanisms for cooling but for heating which is included in the ODE, the heating terms are usually a combination of two terms, Joule heating which is given by the usual  $I_{\text{app}}^2 R$  term or a “heat of polarisation” term which is the voltage loss multiplied by the applied current. Sometimes reversible heating is included which may result in nonlinear governing equations.

There have been a number of approaches to include geometric effects, a notable example is the spiral geometry of the cell with cylindrical batteries, eg. [16, 17, 18, 19]. These models make the assumption of an Archimedean spiral, it is generally noted that spiral geometry leads to an enhanced thermal conductivity. Quantitative estimates of this effect are reported in [19].

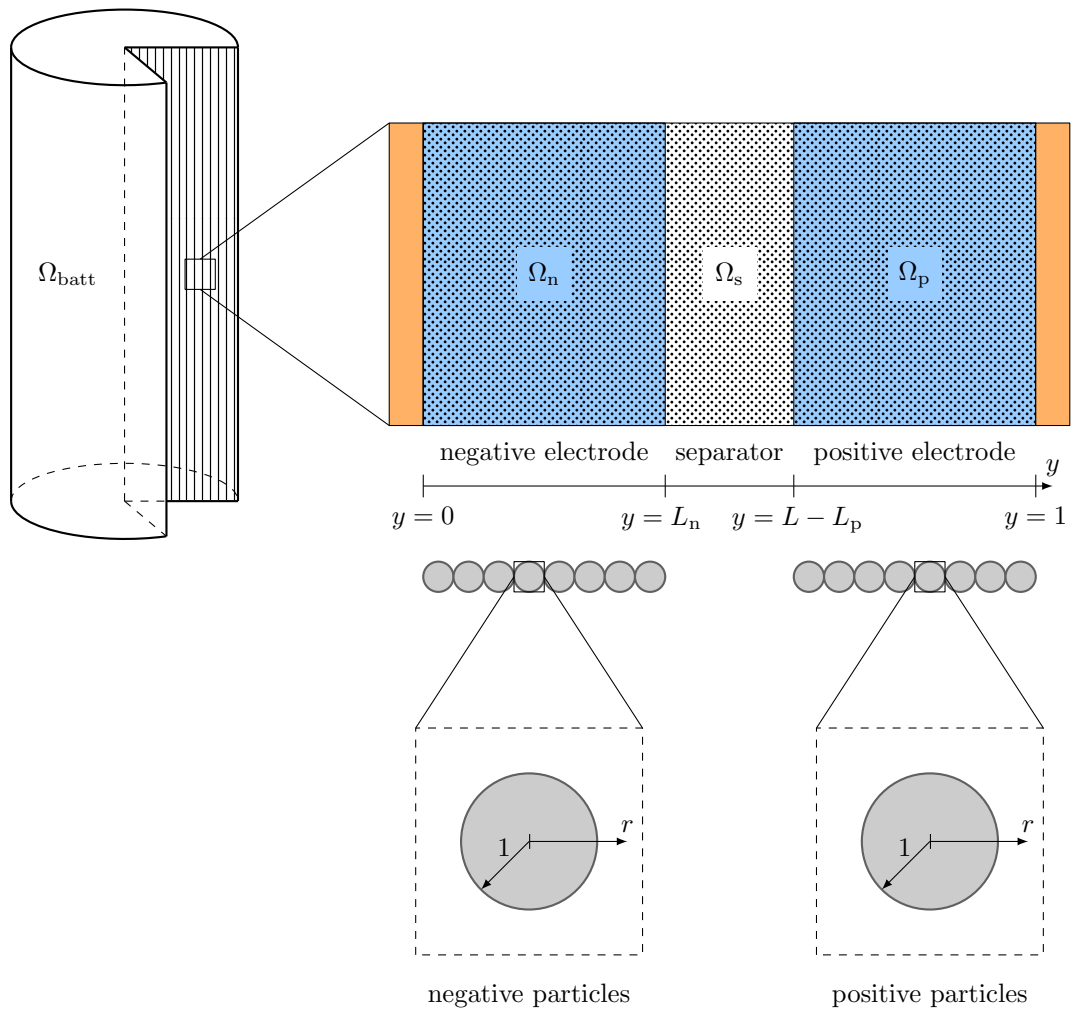


Figure 2: Illustration of the various scales and domains involved in the thermal DFN model (reproduced from [12]).

### 1.3. A brief description of the model

The model described in this article is a reduced order model of the more comprehensive model derived in [11] based on the analysis of the DFN model in [1]. One of main premises of the model is that the rate of diffusion in the electrolyte to the total discharge time is very small ( $\sim 10^{-3}$ ) and this allows the reduction of the full thermal model and even removing one of the scales involved. Two other assumptions which are important is high conductivity in the electrode and the electrolyte. The resulting model has equations for the concentration of lithium in the electrode particles and the temperature distribution in the macroscale. It is noteworthy that the applied current plays the role of a time-dependent parameter in single-particle models like in [1]. In our model the applied current is represented in the form of a time-dependent constraint.

## 2. Dimensionless Single Particle Model with Temperature distribution

The model accounts for the evolution of lithium concentration, electric potentials and temperature on two different scales with associated variables

**Macroscale**  $x \in \Omega_{\text{batt}}$  position in battery,

**Microscale**  $r \in [0, 1]$  distance from centre of electrode particle.

The assumptions mentioned in the previous section allow for the analytical solution of all variables in the mesoscale. Only the remaining equations in the microscale and macroscale are required to be solved numerically.

### 2.1. Evolution of the battery temperature profile

The temperature in the macroscale  $T(x, t)$  is determined by the diffusion equation

$$\partial_t T = \kappa \nabla_x^2 T + Q \quad \text{in } \Omega_{\text{batt}}, \quad (1)$$

where  $Q$  denotes the heat source and  $\kappa$  is the thermal diffusivity. There are two geometries which are of interest, cylindrical and slab, and the use of the Laplacian covers both cases. To model specific situations equation (1) needs to be supplemented with suitable initial and boundary conditions.

The heat source  $Q$  is the sum of of Ohmic heating in electrode particles and electrolyte  $Q_{\text{Ohmic}}$ , and reversible and irreversible heating from the intercalation reaction ( $Q_{\text{irr}}$  and  $Q_{\text{rev}}$ , respectively):

$$Q = Q_{\text{Ohmic}} + Q_{\text{irr}} + Q_{\text{rev}}. \quad (2)$$

Ohmic heating accounts for the electric resistance of the electrodes, and is given by

$$Q_{\text{Ohmic}} = \alpha i^2,$$

where  $i$  represents the local applied current density which has to be calculated and the value of  $\alpha$  is determined in Section 3.2 to be an exceptionally small contribution to the heat source, so

we can effectively set  $\alpha = 0$ . The formulae for reversible and irreversible heating are

$$\begin{aligned} Q_{\text{rev}} &= (\Pi_n - \Pi_p) i, \\ Q_{\text{irr}} &= \frac{2(1 + \gamma T) i}{|\Omega_{\text{cell}}|} \left[ \text{arsinh} \left( \frac{i}{j_0 L_n} \right) + \text{arsinh} \left( \frac{i}{j_0 L_p} \right) \right]. \end{aligned}$$

The function  $j_0$  is called the exchange current density and defined by  $j_0 = \mu[(1 - c_s)c_s c_e]^{\frac{1}{2}}$ . The two closing conditions are

$$\nabla_x V = 0 \quad \text{in } \Omega_{\text{batt}}, \quad (3)$$

$$\int_{\Omega_{\text{batt}}} i(r, t) A(r) dr = I_{\text{app}}(t), \quad (4)$$

where  $i(r)$  is the current density of the mesoscale cell with distance  $r$  from the centre,  $A(r)$  is the current collector area of the corresponding layer  $A(r) = 2\pi h \lceil \frac{r}{h} \rceil$  and  $I_{\text{app}}$  is the total current applied to the battery.

The meaning of (4) is that the volume integral of the current density yields  $I_{\text{app}}$ , the total applied current. From a physical perspective equation (4) is the conservation of charge. The layers are treated as they are in parallel, this implies that the terminal voltage,  $V$ , across the cell will be the same for all layers.

Thanks to (3) the value of terminal voltage only depends on time, ie  $V = V(t)$ . Within the framework of our first order approximation the terminal voltage is decomposed into a leading order value plus a correction,

$$V(t) = V^0(t) + \varepsilon V^1(t).$$

The value of  $V^1$  is given by the formula (34), the leading order voltage  $V^0$  and the current density  $i$  are determined by via charge conservation (4) and the requirement

$$V^0 = \Phi_s^0(y = 1) - \Phi_s^0(y = 0), \quad (5)$$

with the convention that the values of the potential  $\Phi_s^0$  are determined by  $i$  via equations (7) and the Butler-Volmer equation

$$\Phi_s^0 = \frac{2}{\lambda} (1 + \gamma T) \text{arsinh} \left( \frac{J^0}{j_0} \right) + U_{\text{OCP}}(c_s|_{r=1}),$$

with  $U_{\text{OCP}}$  being the open-circuit potential.

## 2.2. Evolution of the lithium concentration in electrode particles

The source terms for the temperature equation require the solution of the mesoscale, which can be done analytically thanks to the asymptotic assumptions. In [20] the modelling in the electrolyte is 1D and this is the approach taken in this article. Then, we have to solve numerically the microscale equations for the lithium concentration in the particles, which read

$$\partial_t c_s = r^{-2} \partial_r (r^2 D_s \partial_r c_s) \quad r \in [0, 1], \quad (6)$$

with boundary and initial conditions:

$$D_s \partial_r c_s = J^0 \quad r = 1, \quad D_s \partial_r c_s = 0 \quad r = 0, \quad c_s(0, r) = 1, \quad (7)$$

where

$$J^0 = \begin{cases} \frac{i}{L_n} & 0 < y < L_n, \\ 0 & L_n < y < 1 - L_p, \\ -\frac{i}{L_p} & 1 - L_p < y < 1, \end{cases}$$

and the parameters  $L_n$  and  $L_p$  represent the relative thickness of the negative and positive electrodes within the cell. This completes the statement of the model.

### 3. Derivation from DFN with Temperature

In this section we demonstrate that the model can be obtained via asymptotic expansion from the standard DFN model with temperature (eg. [11] for a suitable choice of geometry). The starting point is the dimensionless model derived in [11]. Note that all parameters except  $\lambda$ ,  $\gamma$ ,  $\varepsilon$  are piecewise constant. The microscale model is the same as [13], [14] and [16]; the derivation mesoscale equations is based on asymptotic homogenisation, a method that aims to capture effects caused by the geometry of the microstructure.

A slightly less involved approach which delivers similar equations is called volume averaging. Here, the coefficients of the coarse grained equations are obtained in a statistical manner which is not necessarily fully consistent with an underlying microscopic model.

The main assumption is that the non-dimensional parameters  $D_e$ ,  $\alpha_e$ ,  $\alpha_s$  and  $\nu$  are large and of roughly of the same size. To model these assumptions those parameters are multiplied by the common scaling factor  $\frac{1}{\varepsilon}$ . We will demonstrate that the effective model in Section 2 captures the limiting behaviour of the solutions up to first order when  $\varepsilon$  is very small.

#### 3.1. Dimensionless DFN model

With the above conventions the dimensionless DFN model with temperature reads as follows.

*Microscale equations*

$$\partial_t c_s = D_s r^{-2} \partial_r (r^2 \partial_r c_s) \quad \text{in } [0, 1], \quad (8)$$

$$-D_s \partial_r c_s = \beta_s J \quad \text{if } r = 1, \quad (9)$$

where  $D_s$  is the diffusion coefficient of lithium in the electrode (which may depend on the concentration itself, space variables, and temperature),  $J$  is the exchange current.

*Mesoscale equations*

$$\beta_e J = \partial_t c_e - \frac{1}{\varepsilon} D_e \nabla_y^2 c_e \quad \text{in } \Omega_{\text{cell}}, \quad (10)$$

$$0 = \partial_y c_e \quad \text{if } y \in \partial\Omega_{\text{cell}}, \quad (11)$$

$$1 = c_e \quad \text{if } t = 0. \quad (12)$$

The exchange current  $J$  and the overpotential  $\eta$  are defined as

$$J = j_0 \sinh\left(\frac{\lambda}{2} \frac{\eta}{1 + \gamma T}\right), \quad (13)$$

$$\eta = \Phi_s - \Phi_e - U_{\text{OCP}}(c_s|_{r=1}), \quad (14)$$

where  $\mu$  is the reaction rate which is governed by the Arrhenius relation [20]. The electric potentials  $\Phi_s, \Phi_e$  are characterised by the equations

$$\varepsilon J = -\alpha_e \partial_y^2 \Phi_e + \nu(1 + \gamma T) \partial_y^2 \log c_e \quad \Omega_{\text{cell}}, \quad (15)$$

$$0 = \partial_y \Phi_e \quad \partial \Omega_{\text{cell}}, \quad (16)$$

$$0 = \Phi_e(0), \quad (17)$$

$$\varepsilon J = \alpha_s \partial_y^2 \Phi_s \quad \Omega_{\text{cell}} \setminus \Omega_s, \quad (18)$$

$$\varepsilon i = -\alpha_s \partial_y \Phi_s \quad \partial \Omega_{\text{cell}}, \quad (19)$$

$$0 = \partial_y \Phi_s \quad \partial \Omega_s, \quad (20)$$

where the parameters  $\alpha_s$  and  $\alpha_e$  may have different values in  $\Omega_p, \Omega_s$  and  $\Omega_n$ .

*Macroscale equations*

$$\partial_t T = \nabla_x \cdot (\kappa \nabla_x T) + Q \quad \text{in } \Omega_{\text{batt}},$$

where

$$Q = Q_{\text{Ohmic}} + Q_{\text{irr}} + Q_{\text{rev}},$$

and

$$Q_{\text{Ohmic}} = \frac{\lambda}{|\Omega_{\text{cell}}|} \int_{\Omega_{\text{cell}}} (\alpha_s |\nabla_y \Phi_s|^2 + \alpha_e |\nabla_y \Phi_e|^2 - \nu(1 + \gamma T) \nabla_y \log c_e \cdot \nabla_y \Phi_e) dy, \quad (21)$$

$$Q_{\text{rev}} = \frac{\lambda}{|\Omega_{\text{cell}}|} \int_{\Omega_{\text{cell}}} J \Pi dy, \quad (22)$$

$$Q_{\text{irr}} = \frac{\lambda}{|\Omega_{\text{cell}}|} \int_{\Omega_{\text{cell}}} J \eta dy. \quad (23)$$

From (18)-(20) we can conclude

$$i = - \int_{\Omega_n} J dy = \int_{\Omega_p} J dy. \quad (24)$$

An important consequence of (10), (11), (12) and (24) is the equation

$$\int_{\Omega_{\text{cell}}} c_e dy = 1.$$



### 3.2. Asymptotic expansion

The goal is to expand the cell voltage

$$V = \Phi_s(1) - \Phi_s(0) = \Phi_s(t, x, y = 1) - \Phi_s(t, x, y = 0)$$

into powers of  $\varepsilon$ , i.e.

$$V = V^0 + \varepsilon V^1 + O(\varepsilon^2), \quad 0 < \varepsilon \ll 1.$$

The main consequence of the high electrolyte conductivity assumption is that the mesoscale equations are eliminated. This holds not only at leading order, but also for the first order corrections.

We expand  $c_s$ ,  $c_e$ ,  $\Phi_s$ ,  $\Phi_e$  in powers of  $\varepsilon$ , i.e.  $c_e = c_e^0 + \varepsilon c_e^1 + O(\varepsilon^2)$  etc. Plugging this Ansatz into the non-dimensional model in Section 3.1 yields the following equations.

Order  $\varepsilon^0$

$$c_e^0 = 1, \tag{25}$$

$$\Phi_e^0 = 0 \tag{26}$$

$$J^0 = \begin{cases} \frac{i(x)}{L_n} & \Omega_p, \\ 0 & \Omega_s, \\ -\frac{i(x)}{L_p} & \Omega_n, \end{cases} \tag{27}$$

$$\Phi_s^0 = \frac{2}{\lambda}(1 + \gamma T) \operatorname{arsinh} \left( J^0 \mu^{-1} [(1 - c_s^0) c_s^0]^{-\frac{1}{2}} \right) + U_{\text{OCF}}(c_s^0), \tag{28}$$

and the PDE

$$\begin{aligned} \partial_t c_s^0 &= D_s r^{-2} \partial_r (r^2 \partial_r c_s^0) && \text{in } \Omega_s, \\ -D_s \partial_r c_s^0 &= J^0 && \text{on } \partial\Omega_s \end{aligned}$$

Note that both the initial and the boundary values of  $c_s^0$  are constant in  $\Omega_n$  and  $\Omega_p$ , therefore  $c_s^0$  only depend on the microscale variable  $r$ , the macroscale variable  $x$  but on the mesoscale variable  $y$ .

Order  $\varepsilon^1$

$$J^0 = D_e \partial_y^2 c_e^1, \quad 0 = \partial_y c_e^1 |_{\partial\Omega_{\text{cell}}} = \int_{\Omega_{\text{cell}}} c_e^1 dy, \tag{29}$$

$$J^0 = \alpha_e \partial_y^2 \Phi_e^1, \quad 0 = \partial_y \Phi_e^1 |_{\partial\Omega_{\text{cell}}} = \Phi_e^1(0), \tag{30}$$

$$J^0 = \alpha_s \partial_y^2 \Phi_s^1, \quad -i = \alpha_s \partial_y \Phi_s^1 |_{\partial\Omega_{\text{cell}}}. \tag{31}$$

From (24) we have that  $\int_{\Omega_p} J^1 dy = \int_{\Omega_n} J^1 dy = 0$ , and by linearity of (8) and (9) one finds that

$$\int_{\Omega_n} c_s^1 dy = \int_{\Omega_p} c_s^1 dy = 0. \tag{32}$$

The solutions of eqns (29), (30) and (31) are given by

$$c_e^1 = \frac{i}{6D_e} (L_p^2 - L_n^2) + \frac{i}{2D_e} \begin{cases} \frac{y^2}{L_n} - 1 + L_n & \text{if } y \in \Omega_n, \\ 2y - 1 & \text{if } y \in \Omega_s, \\ -\frac{1}{L_p}(y-1)^2 + 1 - L_p & \text{if } y \in \Omega_p, \end{cases}$$

$$\Phi_e^1 = \frac{i}{2\alpha_e} \begin{cases} \frac{y^2}{L_n} & \text{if } y \in \Omega_n, \\ 2y - L_n & \text{if } y \in \Omega_s, \\ -\frac{1}{L_p}(y-1)^2 + 2 - L_n - L_p & \text{if } y \in \Omega_p, \end{cases}$$

$$\Phi_s^1 = \frac{i}{2\alpha_s} \begin{cases} \bar{\Phi}_{s,n}^1 + \frac{1}{L_n}(y - L_n)^2 & \text{if } y \in \Omega_n, \\ \bar{\Phi}_{s,p}^1 - \frac{1}{L_p}(y - 1 + L_p)^2 & \text{if } y \in \Omega_p, \end{cases}$$

such that

$$\bar{c}_{e,n}^1 = \frac{1}{|\Omega_n|} \int_{\Omega_n} c_e^1 dy = \frac{i}{6D_e} (L_p^2 - L_n^2 - 4L_n + 3),$$

$$\bar{c}_{e,p}^1 = \frac{1}{|\Omega_p|} \int_{\Omega_p} c_e^1 dy = \frac{i}{6D_e} (L_p^2 - L_n^2 + 4L_p - 3),$$

$$\bar{\Phi}_{e,n}^1 = \frac{1}{|\Omega_n|} \int_{\Omega_n} \Phi_e^1 dy = \frac{L_n}{6\alpha_e}$$

$$\bar{\Phi}_{e,p}^1 = \frac{1}{|\Omega_p|} \int_{\Omega_p} \Phi_e^1 dy = \frac{1}{6\alpha_e} (6 - 4L_p - 3L_n)$$

The values of  $\bar{\Phi}_s^1$  on  $\Omega_p$  and  $\Omega_n$  are determined by (24):

$$\begin{aligned} 0 &= \frac{1}{|\Omega_n|} \left( \int_{\Omega_n} J dy - i \right) \\ &= \frac{\varepsilon}{2|\Omega_n|} \int_{\Omega_n} \left[ \frac{c_e^1}{c_e^0} + \frac{1 - 2c_s^0}{(1 - c_s^0)c_s^0} c_s^1 \right. \\ &\quad \left. + \frac{\lambda}{1 + \gamma T} \coth\left(\frac{\lambda}{2} \frac{\eta^0}{1 + \gamma T}\right) (\bar{\Phi}_s^1 - \bar{\Phi}_e^1 + U'_{\text{OCP}}(c_s^0) c_s^1) \right] J^0 dy + O(\varepsilon^2) \\ &= \frac{\varepsilon}{2} \left[ \bar{c}_{e,p}^1 + \frac{\lambda}{1 + \gamma T} \coth\left(\frac{\lambda}{2} \frac{\eta^0}{1 + \gamma T}\right) (\bar{\Phi}_s^1 - \bar{\Phi}_e^1) \right], \end{aligned} \quad (33)$$

and analogous for  $\Omega_n$ . The terms involving  $c_s^1$  drop out thanks to (32). This implies that

$$\begin{aligned} \bar{\Phi}_s^1 &= \bar{\Phi}_e^1 - \frac{1}{\lambda} (1 + \gamma T) \tanh\left(\frac{\lambda}{2} \frac{\eta^0}{1 + \gamma T}\right) \bar{c}_e^1 \\ &= \bar{\Phi}_e^1 - \frac{1}{\lambda} (1 + \gamma T) \left( 1 + \sinh^{-2}\left(\frac{\lambda}{2} \frac{\eta^0}{1 + \gamma T}\right) \right)^{-\frac{1}{2}} \bar{c}_e^1 \\ &= \bar{\Phi}_e^1 - \frac{1}{\lambda} (1 + \gamma T) \left( 1 + \frac{1}{i^2} (1 - c_s^0) c_s^0 \right)^{-\frac{1}{2}} \bar{c}_e^1. \end{aligned}$$

Putting the results of these calculations together we obtain the correction term

$$\begin{aligned}
V^1 &= \Phi_s^1(1) - \Phi_s^1(0) = \frac{i}{2\alpha_s} (\bar{\Phi}_{s,p}^1 - \bar{\Phi}_{s,n}^1 - L_p - L_n) \\
&= \frac{i}{2\alpha_s} \left[ \frac{1}{\alpha_e} \left( 1 - \frac{2}{3}(L_p - L_n) \right) - L_p - L_n \right. \\
&\quad + \frac{1}{\lambda}(1 + \gamma T) \left( \left( 1 + \frac{1}{i^2}(1 - c_{s,n}^0) c_{s,n}^0 \right)^{-\frac{1}{2}} \frac{i}{6D_e}(L_p^2 - L_n^2 - 4L_n + 3) \right. \\
&\quad \left. \left. - \left( 1 + \frac{1}{i^2}(1 - c_{s,p}^0) c_{s,p}^0 \right)^{-\frac{1}{2}} \frac{i}{6D_e}(L_p^2 - L_n^2 + 4L_p - 3) \right) \right]. \tag{34}
\end{aligned}$$

Note that  $V^1$  does not depend on  $x$ , but  $i$  and  $c_s^0$  are functions of  $x$ . To evaluate (34) one can choose an arbitrary point  $x \in \Omega_{\text{batt}}$ .

It is now possible to compute the heat source for the macroscale. The heat source will be different depending on the region of the cell it is in. The heat source in each region is given by

$$\begin{aligned}
Q_s &= \frac{\lambda\alpha_s}{|\Omega_{\text{cell}}|} \int_{\Omega_{\text{cell}}} |\partial_y \Phi_s|^2 dy \\
&= \frac{\lambda\alpha_s}{|\Omega_{\text{cell}}|} \int_{\Omega_{\text{cell}}} (0 + \varepsilon \partial_y \Phi_s^1)^2 dy \\
&= \frac{\lambda\alpha_s \varepsilon^2}{|\Omega_{\text{cell}}|} \int_{\Omega_{\text{cell}}} (\partial_y \Phi_s^1)^2 dy.
\end{aligned}$$

A similar calculation can be carried out for  $Q_e$  and so the heat source term due to Ohmic heating is negligible as compared to the reversible and irreversible heating. In [15], much of the input from the electrochemical part of the model is the “ $I_{\text{app}}^2 R$ ”, as shown here, this is a relative small effect compared to other effects. It may be expected that models which essentially use just Ohmic heating as a source term will likely give poor predictions. The only function of  $y$ , the mesoscale variable is  $c_e$  which appears in the function  $j_0 = K \sqrt{c_s - c_s^2} \sqrt{1 + \varepsilon c_e^1}$ , where  $K$  is the reaction rate, which is dependent upon the temperature. So we expand the mesoscale heat source term to  $O(1)$  and integrate over the cell getting:

$$Q_{\text{irr}} = \frac{2(1 + \gamma T)}{|\Omega_{\text{cell}}|} \left[ L_n \operatorname{arsinh} \left( \frac{i}{j_0 L_n} \right) + L_p \operatorname{arsinh} \left( \frac{i}{j_0 L_p} \right) \right], \tag{35}$$

#### 4. Conclusions

In this work, we have provided a coupled thermal-electrochemical model which captures the temperature distribution across the battery. The model has been formally derived from the fully coupled thermal Doyle-Fuller-Newman model which involves three very distinct scales: battery, cell and particle. Using asymptotic methods we reduced the full model taking the assumptions of fast diffusion of ions in the electrolyte, and high conductivity both in the electrodes and

the electrolyte. These assumptions allow us to solve analytically at the mesoscale (cell level) leaving only the temperature at the macroscale (battery level) and lithium concentration at the microscale (particle level) to be solved numerically. The resulting model, which belongs to the family of Single Particle Models, captures the behaviour of the battery at three different scales with a similar computational cost to the isothermal Doyle-Fuller-Newman model. This simple model, even though it is still too complex to be implemented in battery management systems, can play a very important role in demanding applications such as battery design and diagnosis.

## 5. Acknowledgements

The authors acknowledge support from the EPSRC Prosperity Partnership (EP/R004927/1) and The Faraday Institution (EP/S003053/1 Grant No. FIRG025).

## Appendix A. Dimensional DFN model

We state the dimensional version of the DFN model with temperature which has been derived in [11]. Dimensional variables and parameters are consistently written with a ‘hat’ (e.g.  $\hat{D}_e$ ) to prevent confusion with dimensionless versions.

### *Microscale equations*

$$\partial_{\hat{t}} \hat{c}_s = \hat{D}_s \nabla_{\hat{z}}^2 \hat{c}_s \quad \text{in } \hat{\Omega}_s, \quad (\text{A.1})$$

$$-\hat{D}_s \nabla_{\hat{z}} \hat{c}_s \cdot \nu_s = \frac{\hat{J}}{aF} \quad \text{on } \partial \hat{\Omega}_s, \quad (\text{A.2})$$

where  $\hat{D}_s$  is the diffusion coefficient of lithium in the electrode (which may depend on the concentration itself, space variables, and temperature),  $\hat{J}$  is the interfacial current,  $a$  is the surface area density and  $F$  is the Faraday constant.

### *Mesoscale equations*

$$\frac{\hat{J}}{F} = \varphi_e \partial_{\hat{t}} \hat{c}_e - \hat{D}_e \nabla_{\hat{y}}^2 \hat{c}_e \quad \text{in } \hat{\Omega}_{\text{cell}} \quad (\text{A.3})$$

$$0 = n \cdot \nabla_{\hat{y}} \hat{c}_e|_{\hat{y} \in \{0, L\}}, \quad (\text{A.4})$$

$$c_{e, \text{init}} = \hat{c}_e|_{\hat{t}=0}. \quad (\text{A.5})$$

The exchange current  $\hat{J}$  and the overpotential  $\hat{\eta}$  are defined as

$$\hat{J} = \begin{cases} a m [(c_s^{\text{max}} - \hat{c}_s) \hat{c}_s \hat{c}_e]^{\frac{1}{2}} \sinh\left(\frac{F}{2R_g T} \hat{\eta}\right), & \hat{\Omega}_{\text{cell}} \setminus \hat{\Omega}_S, \\ 0 & \hat{\Omega}_S \end{cases} \quad (\text{A.6})$$

$$\hat{\eta} = \hat{\Phi}_s - \hat{\Phi}_e - \hat{U}_{\text{eq}}(\hat{c}_s). \quad (\text{A.7})$$

The electric potentials  $\hat{\Phi}_s, \hat{\Phi}_e$  are characterised by the equations

$$\hat{J} = -\sigma_e \nabla_{\hat{y}}^2 \hat{\Phi}_e + 2(1-t^+) \sigma_e \frac{R_g T}{F} \nabla_{\hat{y}}^2 \log \hat{c}_e \quad \hat{\Omega}_{\text{cell}}, \quad (\text{A.8})$$

$$0 = n \cdot \nabla_{\hat{y}} \hat{\Phi}_e \quad \partial \hat{\Omega}_{\text{cell}}, \quad (\text{A.9})$$

$$0 = \hat{\Phi}_e(0), \quad (\text{A.10})$$

$$\hat{J} = \sigma_s \nabla_{\hat{y}}^2 \hat{\Phi}_s \quad \hat{\Omega}_{\text{cell}} \setminus \hat{\Omega}_S \quad (\text{A.11})$$

$$\mp \varepsilon \hat{I} = \sigma_s n \cdot \nabla_{\hat{y}} \hat{\Phi}_s \quad \partial \hat{\Omega}_{\text{cell}}, \quad (\text{A.12})$$

$$0 = n \cdot \nabla_{\hat{y}} \hat{\Phi}_s \quad \partial \hat{\Omega}_S, \quad (\text{A.13})$$

where the parameters  $\sigma_s$  and  $\sigma_e$  may have different values in  $\hat{\Omega}_p, \hat{\Omega}_S$  and  $\hat{\Omega}_n$ .

*Macroscale equations*

$$\theta \partial_{\hat{t}} \hat{T} = \nabla_{\hat{x}} \cdot \left( \hat{\kappa} \nabla_{\hat{x}} \hat{T} \right) + Q,$$

where

$$Q = Q_{\text{Ohmic}} + Q_{\text{irr}} + Q_{\text{rev}}$$

and

$$\begin{aligned} Q_{\text{Ohmic}} &= \frac{1}{\|\hat{\Omega}_{\text{cell}}\|} \int_{\hat{\Omega}_{\text{cell}}} \left( \sigma_s \|\nabla_{\hat{y}} \hat{\Phi}_s\|^2 + \sigma_e \|\nabla_{\hat{y}} \hat{\Phi}_e\|^2 - 2(1-t^+) \sigma_e \frac{R_g T}{F} \nabla_{\hat{y}} \log \hat{c}_e \cdot \nabla_{\hat{y}} \hat{\Phi}_e \right) dx, \\ Q_{\text{rev}} &= \frac{1}{\|\hat{\Omega}_{\text{cell}}\|} \int_{\hat{\Omega}_{\text{cell}}} \hat{J} \hat{\Pi} dx, \\ Q_{\text{irr}} &= \frac{1}{\|\hat{\Omega}_{\text{cell}}\|} \int_{\hat{\Omega}_{\text{cell}}} \hat{J} \hat{\eta} dx. \end{aligned}$$

We define the following scalings of the problem

$$\begin{aligned} \hat{t} &= t_0 t, & \hat{c}_s &= c^{\max} c_s, & \hat{\Phi}_s &= \Phi_0 \Phi_s, & \hat{J} &= \frac{I_0}{L} J, \\ \hat{z} &= Rz, & \hat{c}_e &= c_{e,\text{init}} c_e, & \hat{\Phi}_e &= \Phi_0 \Phi_e, & \hat{I} &= I_0 I, \\ \hat{y} &= Ly, & \hat{\eta} &= \Phi_0 \eta, & \hat{U}_k &= \Phi_0 U_k, & \hat{T} &= \frac{R_g T_{\text{amb}} c_n^{\max}}{\theta} T + T_{\text{amb}}, \\ \hat{x} &= L_{\text{batt}} x, & \Omega_{\text{batt}} &= L_{\text{batt}} \hat{\Omega}_{\text{batt}}, & \Pi &= \frac{R_g T_{\text{amb}}}{F} \hat{\Pi}, & \hat{Q} &= \frac{i_0 R_g T_{\text{amb}}}{LF} Q, \end{aligned} \quad (\text{A.14})$$

where  $t_0 = F c_n^{\max} L / I_0$ . Note that some of the dimensional parameters here, such as  $R, \varphi_e, \sigma_s$  or  $c^{\max}$ , are piecewise constant to capture the different properties of each electrode and the separator.

The parameters of the dimensionless DFN model in section 2 are given by

$$\begin{aligned}
\alpha_s &= \frac{\sigma_s \Phi_0}{LI_0}, & \alpha_e &= \frac{\sigma_e \Phi_0}{LI_0}, & \beta_s &= \frac{I_0 t_0}{a R F c^{\max} L}, & \beta_e &= \frac{I_0 t_0 (1 - t^+)}{\varphi_e F c_{e, \text{init}} L}, \\
D_s &= \frac{\hat{D}_s t_0}{R^2}, & D_e &= \frac{\hat{D}_e t_0}{\varphi_e L^2}, & \gamma &= \frac{\Delta T}{T_{\text{amb}}}, & \mu &= \frac{a m c^{\max} \sqrt{c_{e, \text{init}} L}}{I_0}, \\
\lambda &= \frac{\Phi_0 F}{R_g T_{\text{amb}}}, & \kappa &= \frac{\hat{\kappa} t_0}{\theta L_{\text{batt}}^2}, & \nu &= 2(1 - t^+) \frac{\sigma_e R_g T_{\text{amb}}}{F L I_0}.
\end{aligned} \tag{A.15}$$

## References

- [1] S. G. Marquis, V. Sulzer, R. Timms, C. P. Please, S. J. Chapman, An Asymptotic Derivation of a Single Particle Model with Electrolyte, *Journal of The Electrochemical Society* 166 (2019) A3693–A3706.
- [2] M. Doyle, T. F. Fuller, J. Newman, Modeling of Galvanostatic Charge and Discharge of the Lithium/Polymer/Insertion Cell, *Journal of The Electrochemical Society* 140 (1993) 1526–1533.
- [3] T. F. Fuller, M. Doyle, J. Newman, Simulation and Optimization of the Dual Lithium Ion Insertion Cell, *Journal of The Electrochemical Society* 141 (1994) 1–10.
- [4] T. F. Fuller, M. Doyle, J. S. Newman, Relaxation Phenomena in Lithium-Ion-Insertion Cells, *Journal of The Electrochemical Society* 141 (1994) 982.
- [5] J. S. Edge, S. O’Kane, R. Prosser, N. D. Kirkaldy, A. N. Patel, A. Hales, A. Ghosh, W. Ai, J. Chen, J. Yang, S. Li, M. C. Pang, L. Bravo Diaz, A. Tomaszewska, M. W. Marzook, K. N. Radhakrishnan, H. Wang, Y. Patel, B. Wu, G. J. Offer, Lithium ion battery degradation: what you need to know, *Physical Chemistry Chemical Physics* 23 (2021) 8200–8221.
- [6] T. Yuksel, S. Litster, V. Viswanathan, J. J. Michalek, Plug-in hybrid electric vehicle lifepo4 battery life implications of thermal management, driving conditions, and regional climate, *Journal of Power Sources* 338 (2017) 49–64.
- [7] D. Worwood, Q. Kellner, M. Wojtala, W. D. Widanage, R. McGlen, D. Greenwood, J. Marco, A new approach to the internal thermal management of cylindrical battery cells for automotive applications, *Journal of Power Sources* 346 (2017) 151–166.
- [8] C.-H. Chen, F. Brosa Planella, K. O’Regan, D. Gastol, W. D. Widanage, E. Kendrick, Development of Experimental Techniques for Parameterization of Multi-scale Lithium-ion Battery Models, *Journal of The Electrochemical Society* 167 (2020) 080534.
- [9] J. Landesfeind, H. A. Gasteiger, Temperature and Concentration Dependence of the Ionic Transport Properties of Lithium-Ion Battery Electrolytes, *Journal of The Electrochemical Society* 166 (2019) A3079–A3097.
- [10] K. O’Regan, F. Brosa Planella, W. D. Widanage, E. Kendrick, Thermal-electrochemical parameters of a high energy lithium-ion cylindrical battery, *Electrochimica Acta* 425 (2022) 140700.
- [11] M. J. Hunt, F. Brosa Planella, F. Theil, W. D. Widanage, Derivation of an effective thermal electrochemical model for porous electrode batteries using asymptotic homogenisation, *Journal of Engineering Mathematics* 122 (2020) 31–57.
- [12] F. Brosa Planella, M. Sheikh, W. D. Widanage, Systematic derivation and validation of a reduced thermal-electrochemical model for lithium-ion batteries using asymptotic methods, *Electrochimica Acta* 388 (2021) 138524.

- [13] W. B. Gu, C. Y. Wang, Thermal-Electrochemical Modeling of Battery Systems, *Journal of The Electrochemical Society* 147 (2000) 2910.
- [14] M. G. Hennessy, I. R. Moyses, Asymptotic reduction and homogenization of a thermo-electrochemical model for a lithium-ion battery, *Applied Mathematical Modelling* 80 (2020) 724–754.
- [15] X. Lin, H. E. Perez, S. Mohan, J. B. Siegel, A. G. Stefanopoulou, Y. Ding, M. P. Castanier, A lumped-parameter electro-thermal model for cylindrical batteries, *Journal of Power Sources* 257 (2014) 12–20.
- [16] T. I. Evans, R. E. White, A Thermal Analysis of a Spirally Wound Battery Using a Simple Mathematical Model, *Journal of The Electrochemical Society* 136 (1989) 2145–2152.
- [17] K. Somasundaram, E. Birgersson, A. S. Mujumdar, Thermal-electrochemical model for passive thermal management of a spiral-wound lithium-ion battery, *Journal of Power Sources* 203 (2012) 84–96.
- [18] M. Guo, R. E. White, Mathematical model for a spirally-wound lithium-ion cell, *Journal of Power Sources* 250 (2014) 220–235.
- [19] S. Psaltis, R. Timms, C. Please, S. J. Chapman, Homogenisation of spirally-wound high-contrast layered materials, *arXiv preprint* (2020).
- [20] G. L. Plett, *Battery Management Systems, Volume 1: Battery Modeling*, Artech House, 2015.